Acta Materialia 96 (2015) 203–211

Contents lists available at ScienceDirect

Acta Materialia

journal homepage: www.elsevier.com/locate/actamat

On the role of zinc on the formation and growth of intermetallic phases during interdiffusion between steel and aluminium alloys

H. Springer *, A. Szczepaniak, D. Raabe

Max-Planck-Institut für Eisenforschung GmbH, 40237 Düsseldorf, Germany

ARTICLE INFO

Article history:
Received 9 February 2015
Revised 8 June 2015
Accepted 13 June 2015

Keywords:
Interdiffusion
Interface
Aluminising
Zinc coatings
Joining

ABSTRACT

The effect of Zn – both within Al and as a coating on steel – on the intermetallic phase formation and growth was systematically studied in controlled experiments, simulating the interfacial reactions taking place in dissimilar solid/solid and solid/liquid joining procedures. Independent from the reaction temperature, the addition of 1.05 at.% Zn (2.5 wt.%) to Al had no effect on the reaction layers' build-up with the η phase (Al_5Fe_2) as the dominant component, but accelerated their parabolic growth up to a factor of 13. While Zn-coatings on steel were found to be beneficial for the regular and even formation of intermetallic reaction zones in solid/liquid joining procedures, their role in solid-state processes was found to be more complex and, if no countermeasures are taken, extremely detrimental to the joint properties. Possible reasons for the Zn-induced growth acceleration are discussed, as well as consequences for possible optimisation steps for reducing harmful effects of Zn in dissimilar joints between Al alloys and steel.

1. Introduction

Dissimilar joining between iron (Fe) based steels and aluminium (Al) alloys is the key to blend the attractive property profiles of these most common structural materials in one hybrid part. Steels are mainly chosen for contributing cost effective strength and high stiffness, Al alloys provide low density, high heat conductivity and excellent corrosion resistance [1]. Examples for such hybrid designs are lightweight body-in-white structures in transportation systems [2,3], protective Al coatings on steel sheets or tubes [4,5], or heat exchangers in energy conversion systems [6,7]. In all those applications an intimate bond between both materials is required, thus necessitating the application of thermal joining procedures opposed to mechanical fasteners such as screws or rivets [8]. Adhesive bondings are typically not only less cost effective, but also require overlapping flanges (which increase weight), are limited in the maximum application temperature and deteriorate the thermal and electrical conductivity [9].

The greatest challenge in the application of thermal joining procedures for the dissimilar joining of steel and Al alloys is the formation of inherently brittle intermetallic reaction layers at the interface. Depending on the reaction conditions determined by the respective joining process (e.g. time/temperature cycle, surface conditions, deformation), the reaction layers are complex in terms of build-up and morphology [10–12]. The η phase (Al_5Fe_2) has been identified as the most prominent component in such dissimilar joints, which is widely acknowledged to be caused by its rapid growth kinetics facilitated by the open and anisotropic crystallographic arrangement [13,14]. This prevalence of the η phase is of great relevance for the dissimilar joining of Al alloys and steel as it has been reported to be one of the most brittle intermetallic phases of the Al–Fe system [15,16]. Many studies have indicated the detrimental effect of growing reaction layers on the mechanical properties and the critical thickness has been found to be in the range of 3 – 10 μm, with different microstructural mechanisms deteriorating the joint strength and ductility [11,17,18]. Consequently, numerous process variations have been developed, both for solid-state joining (e.g. friction welding, diffusion bonding etc. [19–21]) and 'solid/liquid' techniques (e. g. Arc- or Laser-processes, where the Al alloy is molten and wets the solid steel [22,23]), all aimed at minimising and controlling the intermetallic layer thickness and build-up to improve the joint properties.

However, the chemical compositions of the reacting alloy systems – i.e. steel, Al alloy and, if used, filler material – have also a pronounced influence on the intermetallic phase formation and growth. The well-known retarding effect of silicon (Si) additions to Al on the growth kinetics of reaction layers is for example long since exploited in Al dip-coatings on steel, even though the mechanism of the growth suppression is still not completely understood [4,10,24,25]. Gebhardt and Obrowski [26] reported that additions

* Corresponding author.
E-mail address: h.springer@mpie.de (H. Springer).

http://dx.doi.org/10.1016/j.actamat.2015.06.028
1359-6454/

of zinc (Zn), on the other hand, have the opposite effect of Si, i.e. leading to rapidly accelerated reaction layer growth up to a factor of more than 50 compared to reactions with pure Al. The growth acceleration was not found to increase linearly with the Zn content, but rather to exhibit a maximum at additions of 10 wt.% Zn [26]. Understanding this effect of Zn is not only important from an academic point of view, but also of enormous technological interest, as Zn-coatings are the most common corrosion protective measures for steels, especially on thin sheet material used in the automotive industry, and thus a common component in the reaction zone in dissimilar Al/steel joints [1]. Many different techniques have been developed to obtain such Zn-coatings, such as galvanic hot dip-coating (as the most commonly applied process), electrolytic deposition, powder/vapour-processes or even organic coatings [27–29]. All of these processes lead to Zn-coatings with thickness values ranging from about five to several hundred μm, and of specific microstructural and chemical characteristics related to the applied treatments. In dip-coating processes for example, small additions of Al (about 0.1 wt.%) are added to the Zn bath, which lead to the formation of a very thin (nm range) layer of an Fe–Al intermetallic reaction layer on the steel substrate [27]. This 'inhibition layer' in between steel and coating is reported to act as a diffusion barrier for Zn, thus suppressing rapid growth of Fe–Zn intermetallic phases ('outbursts') during galvanising, which have been found to strongly decrease the bond quality [30]. Apart from being coincidentally present in the reaction zone stemming from a steel coating during welding, Zn may also be utilised as an alloying element to contribute its cathodic effect for novel Al-based protective coatings on steel [29].

In light of the large variety of joining processes and respective parameters, base materials and types of coatings, it becomes clear that systematic investigations of the underlying phenomena for the intermetallic phase formation and growth are of great interest in order to derive guidelines for the knowledge-based optimisation of dissimilar joining and coating technology.

2. Objective

The objective of this work is to elucidate the role of Zn on the formation and growth of intermetallic reaction layers formed at the interface between steel and Al alloys at elevated temperatures as present in thermal joining procedures. The reaction products are studied in controlled experiments concerning the reaction between pure as well as Zn-containing Al and low C steel with and without different types of Zn-coatings in direct comparison, in experiments above and below the melting point of Al.

3. Materials and methods

3.1. Interdiffusion experiments

The steel samples used for the present study were cut from 3 mm thick sheets of a low-carbon steel (0.08 wt.% C), as used in the automotive industry (type DC04). Three types of steel surface conditions were investigated, namely (i) uncoated, (ii) dip-coated, termed '+Z', and (iii) electrolytic-coated, termed '+ZE'. Two Al alloys were used, namely high purity Al 99.99 as well as Al containing 1.05 at.% Zn (equals 2.5 wt.%), respectively.

Interdiffusion experiments below the melting point of Al were carried out as solid-state diffusion couples. Al samples of $5 \times 5 \times 5$ mm^3 and steel samples of $3 \times 5 \times 7$ mm^3 were cut by spark erosion. The contacting surfaces were ground and polished to a 1 μm finish except for the Zn-coated steel, which was not ground but only polished for 15 s not to remove the coating. After cleaning in an ultrasonic bath of ethanol and acetone, the samples were clamped together and annealed under Ar-atmosphere at temperatures in the range of 400–640 °C for 1–16 h, respectively. Cooling to room temperature was performed at air.

Experiments with liquid Al alloys were performed as dip-tests. Steel samples of $130 \times 30 \times 3$ mm^3 were cut by spark erosion, the surfaces of the uncoated steel ground to 4000 grit, and all specimens cleaned in an ultrasonic bath and thermocouples were attached. The steel sheets were then immersed in Al bath (2 kg charge weight heated by an induction coil) at 750 °C, for 15, 30 and 60 s under an Ar-atmosphere of 400 mbar, and left to cool to room temperature at air afterwards. The steel sheets were pre-heated to 200 °C before immersion by holding them above the melt for 30 s; they reached the experimental temperature within less than 3 s after immersion.

3.2. Characterisation of the reaction zones

Cross sections of the interdiffusion experiments were prepared with standard metallographic techniques. The reaction layers were investigated using optical microscopy (OM; Leica DM4000M) for thickness measurements using a methodology detailed elsewhere [10], and scanning electron microscopy (SEM; Jeol 6450F) for chemical analysis (EDAX energy dispersive X-ray spectroscopy system; EDX) and phase identification (TSL electron backscatter diffraction system; EBSD). Transmission electron microscopy (TEM, Jeol 2200 FS) was performed to characterise the Zn coatings prior to the interdiffusion experiments. Site specific TEM sample preparation was carried out with a focussed ion beam system (FIB, FEI Helios Nano Lab 600i dual beam with Omni Probe manipulator).

4. Results

4.1. Reactions between steel and solid Al alloys

Examples of SEM analysis results from reaction zones formed during interdiffusion between uncoated steel and the Al–Zn alloy at 600 °C are compiled in Fig. 1. Independent from the reaction time, the intermetallic phase seam is protruding finger-shaped into the steel and finely serrated towards the Al alloy (Fig. 1 a and b). EBSD investigations (phase map with image quality data superimposed in grey scale, Fig. 1c) reveal the η phase (green) as its main component, with large columnar grains having grown along the *c*-axis of the phase, as indicated by green and blue colour-coding in the inverse-pole figure map (right image in Fig. 1c). The much thinner seam between the η phase (right image of Fig. 1a) and the adjacent Al-alloy could be identified as the θ phase ($Al_{13}Fe_4$, red in Fig. 1c) which grew from about 6 to about 11 μm between 1 and 16 h reaction time, while the thin layers between η and steel (white arrows in right image of Fig. 1b) most probably consist of the β′ phase (AlFe) and κ carbide (Fe_3AlC) as shown elsewhere [10]. The formation of pores between η and θ phase layers, the volume fraction of which is increasing with reaction time, can be linked to the Kirkendall-effect during growth of the η phase [11,31]. EDX measurements (Fig. 1d) revealed only traces of Zn incorporated in the θ phase, while the η phase contains about 0.5 at.% close to the Al alloy and about 5 at.% at the interface with steel. In view of the small concentrations and the complex morphology of the intermetallic phase seam, it should be noted that probing the exact chemical composition, especially close to the interfacial regions, requires different techniques such electron probe micro analysis or atom probe tomography. Thickness measurements as function of reaction time (Fig. 2a) showed the intermetallic phase seam to exhibit parabolic growth kinetics with a

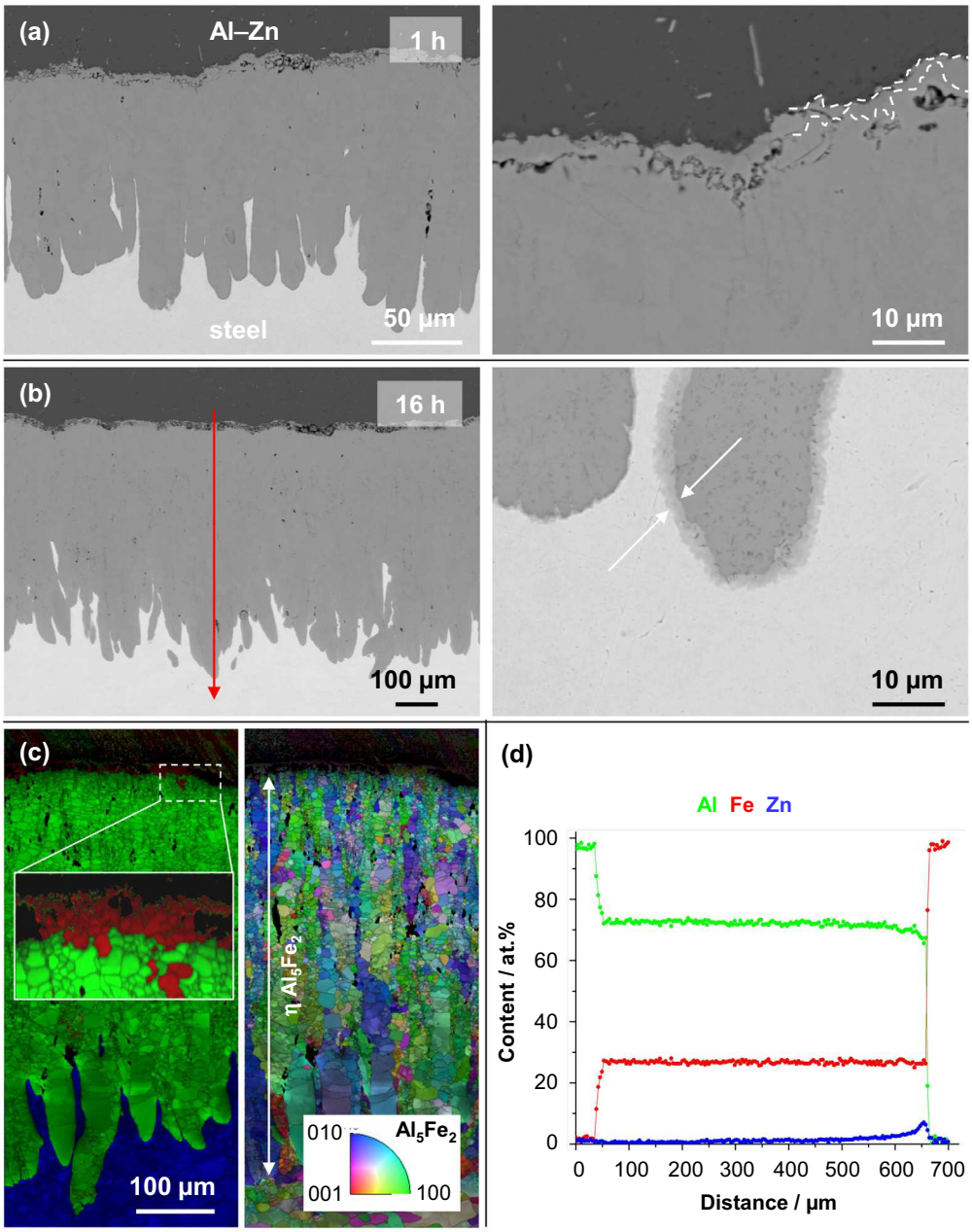

Fig. 1. SEM investigations of the reaction zones from interdiffusion experiments between uncoated steel and Al containing 2.5 wt.% Zn at 600 °C: (a and b) micrographs at different magnification for 1 h and 16 h reaction time, respectively. (c) EBSD analysis for 16 h reaction time with image quality data superimposed in grey scale: Phase mapping (left) with the η phase (Al_5Fe_2) in green, θ phase ($Al_{13}Fe_4$) in red, Al in yellow and Fe α in blue. Corresponding inverse pole figure map (right). (d) EDX line scan result (16 h reaction time) obtained along the red arrow in (b). (For interpretation of the references to colour in this figure legend, the reader is referred to the web version of this article.)

corresponding growth coefficient k of 2.56 µm $s^{-0.5}$, which represents an acceleration of about a factor of 13 compared to experiments with pure Al [10]. The η phase remained the dominant component throughout while both θ and β′/κ layers where found to change little over the chosen time scale. Growth of the intermetallic reaction layers took mainly place towards the Al–Zn alloy, with only about a quarter of the total thickness having grown into the steel relative to the original interface. Corresponding interdiffusion experiments at 560 and 640 °C for 16 h yielded reaction layers that are 67 and 638 µm thick, respectively (Fig. 2b and c). Assuming parabolic growth, this results in growth coefficients k of 0.28 and 2.66 µm $s^{-0.5}$, respectively. The morphology, build-up and relative phase fractions of the reaction layers was not affected by the deviating temperatures.

Prior to interdiffusion experiments with Zn-coated steels, the two coating types chosen here were examined as shown in Fig. 3. Both electrolytical deposition (+ZE, Fig. 3a) and galvanic dip-coating (+Z, Fig. 3b) led to coatings with a similar and regular thickness of about 8–10 µm. TEM investigations of the interface between Zn-coating and steel substrate revealed a thin (about 200 nm) seam consisting of a Fe–Al intermetallic seam in case of the +Z-coating (Fig 3b). While no effort was made to characterise it in this study in more detail, previous investigations have shown this ‘inhibition layer’ to consist of the η phase [27,32].

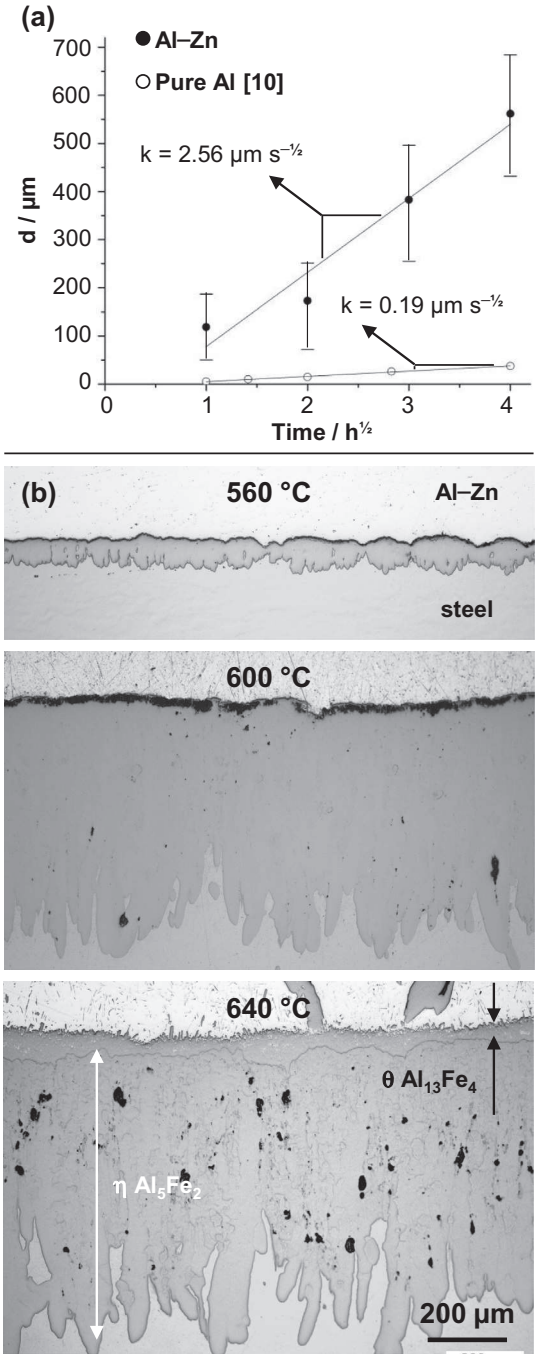

Fig. 2. (a) Thickness data from interdiffusion experiments between uncoated steel and Al containing 2.5 wt.% Zn at 600 °C plotted as a function of reaction time, together with literature data for corresponding experiments with pure Al [10]. (b) Optical micrographs of the reaction layers formed between uncoated steel and Al containing 2.5 wt.% Zn at various temperatures and 16 h reaction time.

Results from interdiffusion experiments between dip-coated steel and pure Al at various temperatures and annealing time are shown in Fig. 4. The reaction zones, whose thickness is increasing with annealing temperature, are much more irregular than in experiments with uncoated steel (Fig. 1). Adjacent to Al the interface of the intermetallic phase seam remains finely serrated, but towards steel no large finger-like protrusions can be observed (Fig. 4a). The intermetallic phase seam is cracked to a large extent and large fractions broke out during metallographic preparation. EDX (Fig. 4b) and EBSD measurements (spot patterns, not shown) indicated the remaining intermetallic seam to consist of the θ phase towards Al and η phase adjacent to steel. Within the θ phase layer no Zn could be detected, but small Al–Zn rich areas in a layered structure, most pronounced for shorter annealing times (Fig. 4c). The η phase contained about 4 at.% Zn, corresponding to the maximum values found for interdiffusion experiments with uncoated steel and Zn-alloyed Al (Fig. 1d). With a thickness of about 95 µm for 600 °C annealing temperature (measured from Al to steel including the fractured area), the reaction zone is considerably larger than respective values obtained with pure Al and uncoated steel (15 µm, [10]), but smaller than with uncoated steel and Zn-containing Al (173 µm, Fig. 2). The Al exhibits pores (white arrows in Fig. 4a) and contains about 1 at.% Zn close to the reaction zones, which only very gradually decreases to less than 0.3 at.% 400 µm away from the reaction zone into the Al base material.

4.2. Reactions between solid steel and liquid Al alloys

Exemplary SEM analysis results from the reaction zones formed between dip-coated steel and Zn containing Al at 750 °C are shown in Fig. 5. Independent from the reaction time, the intermetallic phase seam is of almost identical morphology as those found in interdiffusion experiments between steel and pure Al [10,14,33], namely with finger-like protrusions into the steel and finely serrated features towards the solidified Al–Zn coating (Fig. 5a). EBSD phase analysis (Fig. 5b) and EDX line scan results (Fig 5c) reveal the phase sequence to be also quasi identical to those of

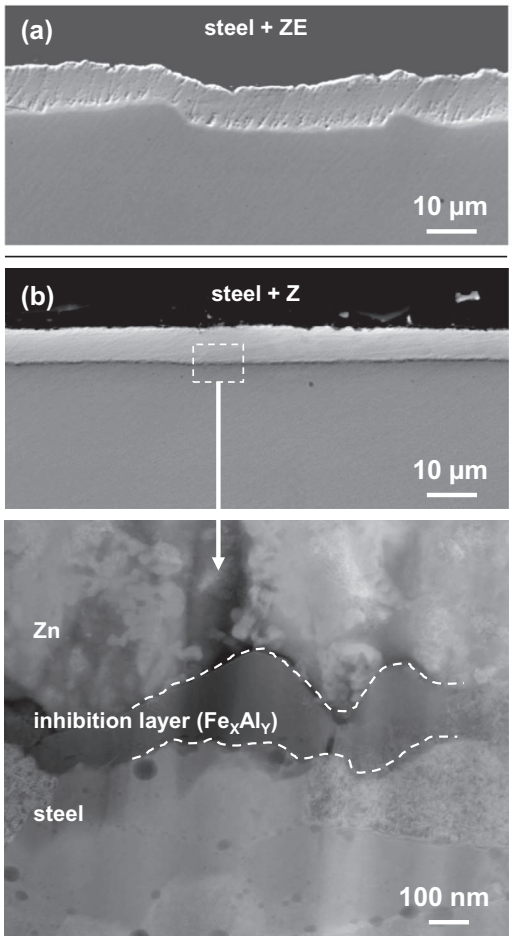

Fig. 3. Analysis of the different Zn-coatings on steel used in this study: (a) SEM micrograph of an electrolytic coating (+ZE). (b) SEM (top) and TEM (STEM HAADF image, bottom) of a galvanic dip-coating (+Z).

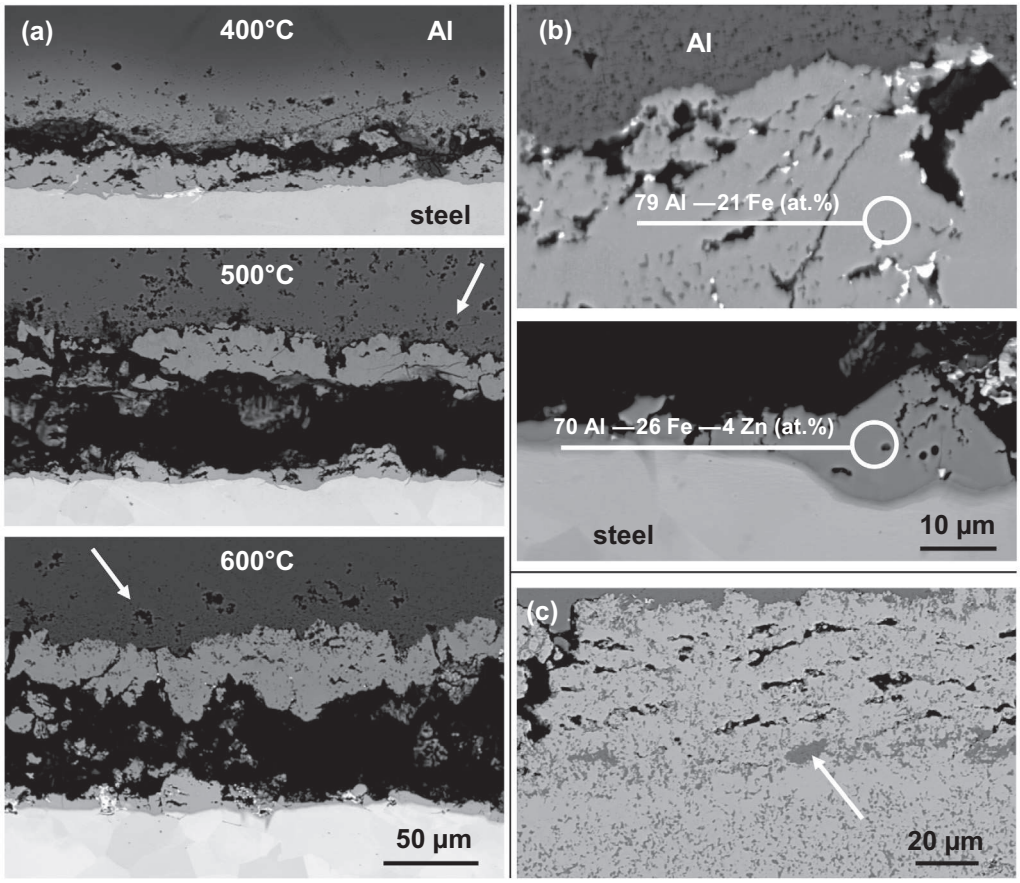

Fig. 4. Results from interdiffusion experiments between pure Al and dip-coated steel (+Z): (a) SEM overview of reaction zones for various temperatures and 4 h reaction time. (b) SEM details of the intermetallic seams adjacent to Al (top) and steel (bottom) formed at 600 °C and 4 h reaction time, white arrows indicating porosity in the Al alloy. Results for respective EDX measurements are indicated in at.%. (c) SEM detail of the intermetallic seam adjacent to Al formed at 600 °C and 2 h reaction time, showing the layered structure of the θ phase ($Al_{13}Fe_4$) with inclusions of Zn-containing Al (white arrow).

respective experiments with pure Al: The dominant component is the η phase (green) adjacent to steel and a thinner θ phase layer (red) in contact with the Al–Zn alloy as well as dispersed within the latter. The η phase contained with between 0.5 and 1 at.% Zn similar amounts as in the solid-state experiments; but the Zn pile-up at the interface towards steel could be observed (with maximum values of about 4 at.%) only sporadic for longer reaction times. Layers of β′ phase and κ carbide could not be detected between the η phase and steel, but may as well be too thin for the applied SEM-based characterisation procedures. Thickness values of the intermetallic phase seam as a function of reaction time are plotted in Fig. 6, together with literature data [33]. In case of Zn-containing Al, a parabolic growth coefficient k of 10.50 µm $s^{-0.5}$ is found (assuming instantaneous growth from the beginning), which represents an acceleration of more than the factor of two compared to reported experimental results for pure Al (k = 4.18 µm $s^{-0.5}$, [33]).

Interdiffusion experiments with liquid pure Al at 750 °C and 30 s reaction time yielded in pronounced differences for the resultant intermetallic reaction layers depending on the type of Zn-coating on the steel substrate (Fig. 7). As shown on the SEM images (top pictures), the reaction layers formed with uncoated steel (Fig. 7a) are slightly thinner but also much more irregular compared to those where Zn-coated steel was used (Fig. 7b and c). The dip coated steel (+Z; Fig. 7c) resulted in the most regular morphology of the reaction layer, and here the η phase crystals have much less sub-grain boundaries perpendicular to their growth direction, especially close to their interface with the θ phase. The phase sequence is unaffected by the type of coating applied.

5. Discussion

5.1. Influence of Zn in Al on the formation and growth of intermetallic phases

The reaction layers formed between low-carbon steel and Al–Zn alloys are quasi identical in terms of build-up and morphology to those formed in interdiffusion experiments with pure Al [10,14,33], with the η phase remaining the dominant component for all investigated interdiffusion temperatures (Figs 1 and 5). The presence of a thin θ phase layer adjacent to the Al–Zn alloy, not only in solid/liquid but now also in the case of solid-state interdiffusion (which was not observed in respective experiments with pure Al [10]), may be explained by the accelerated growth of reaction layers with Al–Zn alloys: As the relative fraction of the θ phase layer in the reaction zone stayed roughly constant throughout our experiments, it seems probable that the θ phase remains too small to be detected in respective experiments with pure Al. The application of high resolution characterisation techniques (such as TEM or atom probe tomography) for its detection is hindered by the mechanically fragile nature of its interface regions induced by Kirkendall porosity [11]. Only negligible amounts of Zn were found

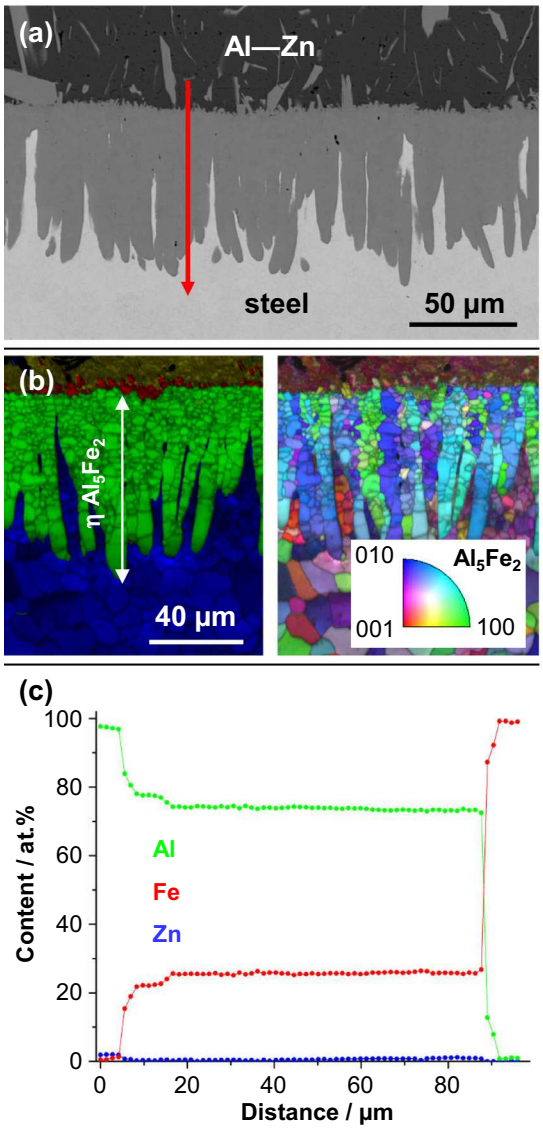

Fig. 5. SEM investigations of the reaction zones from interdiffusion experiments between dip-coated steel (+Z) and Al containing 2.5 wt.% Zn at 750 °C and 30 s reaction time: (a) Micrograph. (b) EBSD analysis with image quality data superimposed in grey scale: Phase mapping (left, colours as in Fig. 1) and corresponding inverse pole figure map (right). (c) EDX line scan result obtained along the red arrow in (a). (For interpretation of the references to colour in this figure legend, the reader is referred to the web version of this article.)

in the θ phase (more in solid/liquid experiments), rendering a possible stabilisation through Zn-incorporation unlikely (Figs). The Zn-content in the η phase is with about 0.5 – 1 at.% less than reported values for the 'inhibition layer' in Zn dip-coatings (more than 22 at.% [32]), but more than in arc-welded joints between Al alloys and Zn-coated steel [23]. Zn pile-up between the η phase and steel (Fig. 1d) is most likely caused by differing diffusion speeds of Zn or it is enriched within the β′/κ phase region. No ternary Al–Fe–Zn phases could be observed, which is expected in light of previous works, where respective compounds were described to form only in the Zn-rich corner of the ternary phase diagram [27,34,35] or as metastable phases [36].

The growth of the reaction layers can be rationalised by parabolic rate laws (Figs. 2 and 6). The observed acceleration compared to experiments with pure Al corroborates the findings reported by Gebhardt and Obrowski [26]. The larger extent of growth acceleration that they reported might have been caused by their specific experimental setup: As no inductive stirring was applied, effects of gravity-induced enrichment of Fe and Zn close to the Al–Zn/Fe interface may have led to overestimated growth rates, which would also explain the layered build-up of the intermetallic phase seam in their experiments [26]. Opposed to what was found for Si-additions to Al [10], increased activation energy for the interdiffusion process seems not to be the reason for the observed growth acceleration in case of Zn-additions (Fig. 8). It should be noted though that possible effects of the different experimental setups (especially the chemical compositions of the base materials) from the literature data plotted in Fig. 8 cannot be ruled out, especially in view of the pronounced experimental scatter induced by the irregular morphology of the intermetallic phase seams. With the exception of Zn incorporation into the η phase as its dominant component, all other possible factors influencing the growth rate (e.g. build-up of the reaction zone, rate law, crystallographic orientation, nucleation conditions) are quasi identical to experiments with pure Al [10,25,37]. While more experiments are clearly required to elucidate the reason for the Zn-induced growth acceleration, the current results hint at an interaction of Zn with the structural vacancies of the η phase [13,14,24], thus facilitating the interdiffusion of Al and Fe through it, as a possible explanation.

5.2. Influence of Zn-coatings on steel on the intermetallic phase formation and growth

In case of solid/liquid interdiffusion, no pronounced difference could be observed in terms of build-up and morphology of the intermetallic reaction layers compared to experiments with uncoated steel (Fig. 7). However, a slightly accelerated growth and more regular reaction zones are present when using Zn-coated steel. This can be explained by the fact that the Zn-coating is quickly dissolved by the liquid Al, leaving a 'clean' steel surface without any contamination such as oxides, ensuring good wetting and thus more regular growth of the reaction layers. The Fe–Al 'inhibition layer' present underneath Zn dip-coatings (Fig. 3) appears to facilitate this phenomenon (growth of pre-nucleated intermetallic phases). The amount of dissolved Zn is small within the inductively stirred Al bath and thus appears to play a minor role; only when the turbulence of the melt is low (and/or the meltpool in welding is small), effects of local enrichment at the interface as described in the previous section might play a role.

In processes where the temperature stays below the melting temperature of Al, however, the role of Zn-coatings on steel appears to be more complex. While it is well established that in solid-state interdiffusion between uncoated steel and Al the

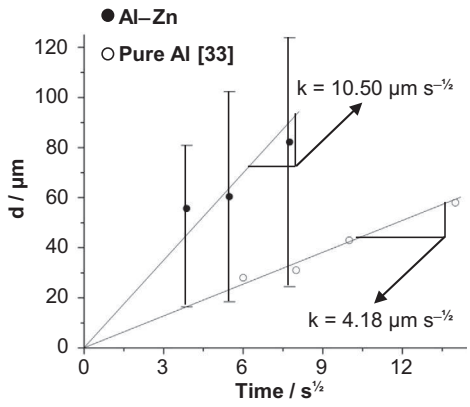

Fig. 6. Thickness data from interdiffusion experiments between dip-coated steel (+Z) and Al containing 2.5 wt.% Zn at 750 °C plotted as a function of reaction time, together with literature data for corresponding experiments with pure Al [33].

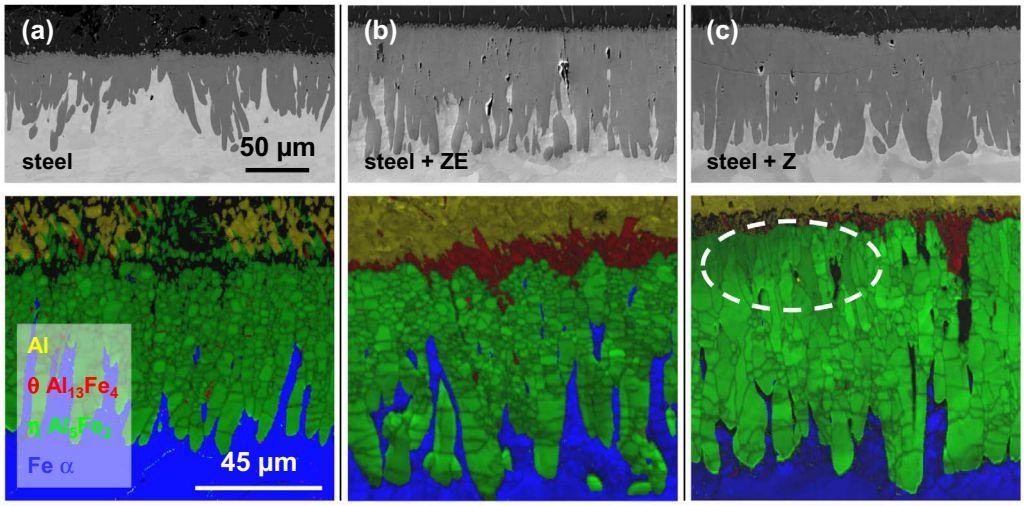

Fig. 7. SEM results from interdiffusion experiments between pure Al and steel with different Zn-coatings at 750 °C and 30 s reaction time. SEM images (top) and EBSD phase/image quality maps (bottom). (a) Without coating, (b) electrolytic coating (+ZE), (c) galvanic dip-coating (+Z).

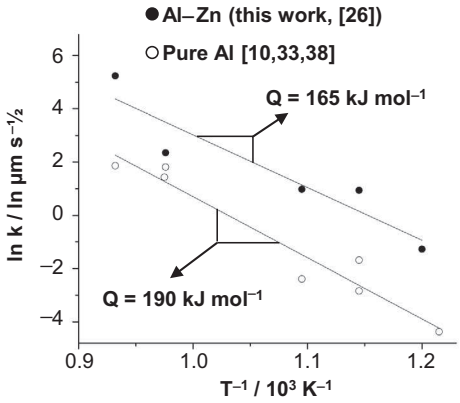

Fig. 8. Arrhenius plot of the rate constants *k* obtained in this study (Figs. 2 and 6) together with literature data [10,26,33,38].

reaction zone consists mainly of the η phase with parabolic, solid-state diffusion controlled growth [10,38], it becomes much larger and exhibits a more complex build-up when Zn-coated steel is used (Fig. 4). Based on theoretical considerations and literature data [34,35,39–41], we propose a scenario of reactions as sketched in Fig. 9 to rationalise our experimental findings: The Zn-coating in between Al and steel (stage i) liquefies at temperatures above the melting point of Zn (419 °C). At lower temperatures melting occurs through the formation of the Zn–Al eutectic (385 °C) as shown in the Al–Zn phase diagram [40]. Zn and Al then readily interdiffuse (stage ii), forming three zones of (a) liquid Zn–Al adjacent to steel, (b) Al with Zn in solid solution and (c) a two phase semi-solid zone of both liquid and solid Al–Zn in between (a) and (b). During holding at the experimental temperature (stage iii), the following processes take place simultaneously: At the interface between steel and the liquefied Al–Zn zone, Fe_XAl_Y intermetallic phases – mainly the η phase – nucleate and grow (in case of dip-coated steel only growth of the pre-nucleated 'inhibition layer'), accelerated by the Zn concentration within Al (parabolic, solid-state interdiffusion). The Fe transported through the growing Fe_XAl_Y seam enriches in the liquid Al–Zn zone, as there is no large meltpool or bath present. As the Zn keeps diffusing into Al, however, its concentration in the liquid zone is lowered (finite amount of Zn determined by the initial coating thickness), which consequently raises the melting temperature of the Al–Zn alloy. The thus shrinking Al–Zn–Fe liquid zone – despite isothermal experimental conditions – decomposes at the moving solidus line into the θ phase and Zn-containing Al in a ternary eutectic reaction [34,35]. Similar effects are well known and exploited in so-called 'transient liquid phase' (TLP) joining procedures [41]. During cooling to room temperature (stage iv) the remaining liquid phase decomposes in a similar manner, leaving behind a microstructure as sketched in Fig. 9. The observed porosity in Al can be explained by both shrinkage of liquid Al–Zn alloys during cooling as well as Kirkendall-porosity [11,31,42]. The θ phase/Al–Zn eutectic formed during cooling – in between the solid-state and constitutively formed products adjacent to the base materials – and is thus most affected by the corresponding stresses, and thereby readily pre-cracked and removed during metallographic preparation, matching our experimental findings (Fig. 4). Future investigations aim at a more detailed understanding and validation of this complex scenario, especially regarding the influence of short joining times and additional effects of mechanical pressure.

5.3. Consequences for the optimisation of bond quality and joining procedures

The excessive formation of inherently brittle intermetallic reaction layers at the interface in dissimilar joining of Al alloys and steel is in general difficult to avoid: once the energy input is high enough to ensure sufficient surface-activation to form a metallic bond, the rapid growth kinetics especially of the η phase quickly result in unsatisfactory thick layers. In view of this narrow processing window the effects of additional elements such as Zn must be critically evaluated to ensure sufficient performance of the hybrid joint.

The addition of Zn along with magnesium – and thus a cathodic corrosion protection – to Al is a promising pathway to develop novel steel dip-coatings for applications in the automotive industry, where the detrimental effects of Zn-coatings on the weldability (high vapour pressure of Zn creating splatters and porosity) represent a strong driving force. The growth accelerating effect of Zn on the intermetallic phases could possibly be compensated by Si additions. The rather large eutectic Si-lamellas, which can deteriorate the coatings ductility [43] and corrosion behaviour [5], could be given a more favourable morphology and dispersion by small additions of strontium or calcium [43,44].

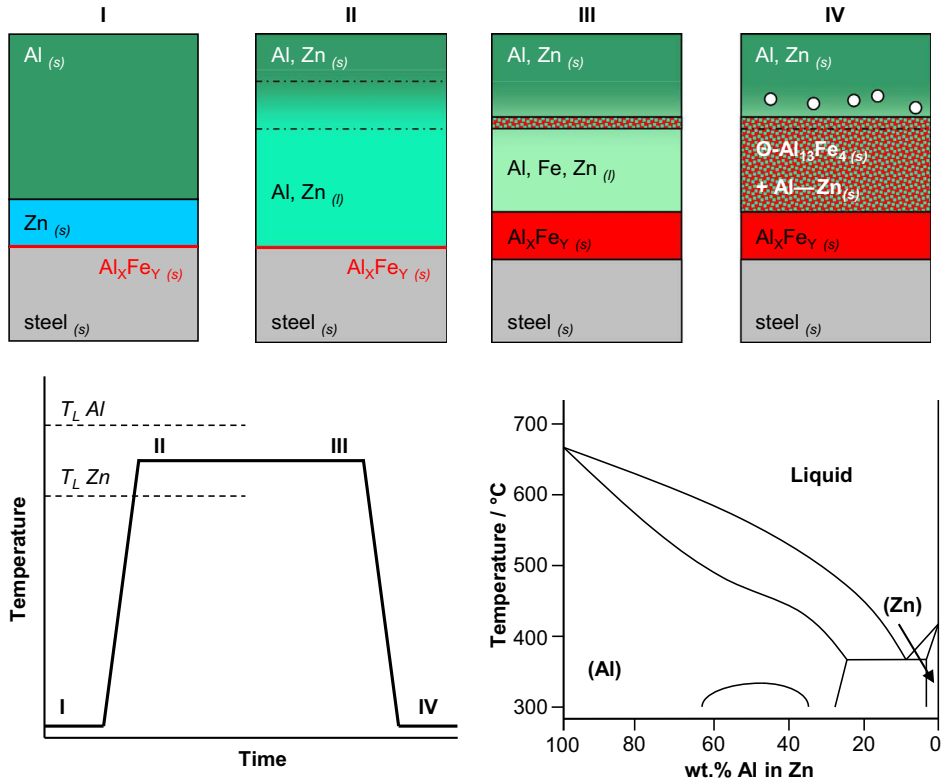

Fig. 9. Suggested reaction scenario for interdiffusion between Zn-coated steel and Al at temperatures between the melting points of Al and Zn, as present in solid-state joining procedures. Phase formation sequence (top) throughout the time/temperature cycle (bottom left), consisting of dissolution of the Zn-coating, formation of liquid, solid and semi-solid Al–Zn zones, and subsequent growth of Al–Fe phases during elevated temperature as well as stemming from decomposition of the liquid zones. Sketch of the Al–Zn phase diagram (bottom right, [40]).

The effects of Zn-coatings on steel, however, are more complex in nature as in case of Zn in Al, depending on the joining setup (e.g. heat input, time/temperature cycle, mechanical influencing factors):

In solid–liquid welding/brazing procedures such as arc and beam processes [22,23] or in hot-dip-aluminising [4,5], where the peak temperatures are relatively high and reaction times are short, Zn-coatings – especially dip-coatings – can be generally regarded as beneficial [45]. Their flux-like behaviour (see Section 5.1) should allow decreasing the thickness of the intermetallic phase seam (e.g. by lower specific heat inputs) without sacrificing its regular morphology and reliable formation. In order to avoid the Zn-induced growth acceleration, the applied Zn-coatings should be as thin as possible, and the joining techniques should enable rapid dispersion of Zn in the molten Al for example by slow welding with large meltpools of strong turbulence.

For joining processes below the melting point of Al the role of Zn-coatings is equivocal. In established rotational friction welding it is typically pushed out of the weld zone during the preheating friction- and the weld-cycles. In friction stir welding (FSW) in a butt joint configuration, sound welds between Zn-coated steel and Al alloys have been produced without interfacial failure [46–48]. Here the tool penetrated the steel only lightly and Zn was apparently scraped by the tool shoulder and mixed into the stir zone, but did not affect the intermetallic phase formation. Another study of FSW in an overlap configuration, where Al is put on top Zn-coated steel, reports that Zn acted beneficial for the bond strength [39]. However, a strong dependence between the bonding strength and failure location and the FSW tool rotation speed was observed in those experiments [39]. These findings can be explained by the reaction scenario proposed in Section 5.2 (Fig. 9): In the initial stage of the joining sequence, the soft and low melting Zn can act as a bonding agent. The presence of a liquid Al–Zn zone ensures intimate contact between both steel and Al even at temperatures where solid-state interdiffusion (and thus formation of a bond) typically does not take place due to impeded nucleation (roughness and contamination of contact surfaces [49,50]). However, if the liquid Al–Zn is not subsequently removed either by material flow (e.g. in FSW) or mechanical pressure (e.g. in resistant spot welding, RP), the described constitutive and solid-state phase formation processes can take place and strongly decrease the bond quality. As these parameters are difficult to control throughout the entire weld region, extremely thin Zn-layers (<1 μm) combined with low temperatures (<500 °C) and medium-to-short joining times promise to result in optimum joint properties.

6. Summary and conclusions

We systematically studied the effect of Zn on the intermetallic phase formation and growth during interdiffusion between steel and Al alloys above and below the melting temperature of Al. The controlled experiments simulate the interfacial reactions present in dissimilar solid–solid and solid–liquid joining procedures. Depending on whether Zn was present as an alloying element within Al or as a coating on steel, strongly differing effects on the intermetallic reaction layers could be observed, and the following conclusions for joining process optimisation can be drawn:

(1) The morphology and build-up of the reaction layers formed between Al containing 1.05 at.% Zn and low carbon steel are practically identical compared to reaction layers formed

with pure Al. The η phase represents the dominant component and contains about 0.5 at.% Zn, with enrichments of up to about 5 at.% close to the interface towards the steel.

(2) Growth of the intermetallic reaction layers formed with Zn-alloyed Al can be described by parabolic rate laws. Also, a pronounced growth-acceleration was observed. The current results render a change in activation energy to be unlikely, and favour an interaction of Zn with the structural vacancies reported for the η phase as a reason for this accelerated growth (up to a factor of 13).

(3) Zn-coatings on steel can be regarded as beneficial in solid–liquid joining procedures, aiding bonding by rapid dissolution and thus a controlled formation of even and regular reaction layers. Local enrichment of Zn to avoid the accelerating effect of Zn should be countered by large and turbulent Al baths or meltpools. Zn-dip-coatings resulted in the most uniform and defect free intermetallic phase seams.

(4) In solid-state joining processes, the role of Zn-coatings on steel is complex and equivocal. While they aid the intimate contact between steel and Al alloy in the early stages of the joint formation, they lead to the formation of extremely detrimental interfacial microstructures if no countermeasures are taken regarding Zn-layer thickness, time/temperature cycle and material flow in the weld region.

(5) Al alloys with additions of Zn, Mg, Si and Sr or Ca represent a promising basis for novel protective steel coatings with optimised mechanical and chemical performance as well as superior weldability compared to established Zn-based coatings.

Acknowledgements

M. Rolf is acknowledged for contributing results from interdiffusion experiments between steel and Zn-containing Al obtained during his bachelor thesis work. M. Palm and F. Stein are gratefully acknowledged for valuable discussions.

References

[1] M.F. Ashby, Materials Selection in Mechanical Design, Butterworth-Heinemann, Burlington, MA, 2005.
[2] U. Dilthey, L. Stein, Sci. Technol. Weld. Joining 11 (2006) 135.
[3] G.A. Young, J.G. Banker. in: Proc 13th Off Shore Symposium, Houston, 2004.
[4] S.G. Denner, R.D. Jones, R.J. Thomas, J. Iron Steel Inst. 48 (1975) 241.
[5] B. Lemmens, Y. Gonzalez Garcia, B. Corlud, J. De Strycker, I. De Graeve, K. Verbeken, Surf. Coat. Technol. (2014), http://dx.doi.org/10.1016/j.surfcoat.2014.06.064.
[6] W.F. Hess, E.F. Nippes, Am. Weld. J. (Research Supplement) (1946) 129.
[7] H. Hartwig, Aluminium 57 (1981) 615.
[8] T.A. Barnes, I.R. Pashby, J. Mater. Process. Technol. 99 (2000) 62.
[9] T.A. Barnes, I.R. Pashby, J. Mater. Process. Technol. 99 (2000) 72.
[10] H. Springer, A. Kostka, E.J. Payton, D. Raabe, A. Kaysser-Pyzalla, G. Eggeler, Acta Mater. 59 (2010) 1586.
[11] H. Springer, A. Kostka, J.F. dos Santos, D. Raabe, Mater. Sci. Eng. A 528 (2011) 4630.
[12] A. Szczepaniak, J. Fan, A. Kostka, D. Raabe, Adv. Eng. Mater. 14 (2012) 464.
[13] K. Schubert, U. Rosler, K. Anderko, L. Harle, Naturwissenschaften 16 (1953) 437.
[14] T. Heumann, S. Dittrich, Z. Metall. 50 (1959) 617.
[15] O. Kubaschewski, Iron – Binary Phase Diagrams, Springer Verlag, Berlin, 1982.
[16] V.R. Ryabov, Aluminizing of Steel, Oxonian Press, New Delhi, 1985.
[17] D.R.G. Achar, J. Ruge, S. Sundaresan, Aluminium 56 (1980) 220.
[18] M. Yilmaz, M. Cöl, M. Acet, Mater. Charact. 49 (2003) 421.
[19] K. Mechsner, H. Klock, Aluminium 59 (1983) 850.
[20] K. Mori, N. Bay, L. Fratini, F. Micari, A.E. Tekkaya, CIRP Ann. 62 (2013) 673.
[21] P. Groche, S. Wohletz, M. Brenneis, C. Pabst, F. Resch, J. Mater. Process. Technol. 214 (2014) 1972.
[22] C.R. Radscheit, Ph.D. Thesis, Universität Bremen, Bremen, Germany, 1996.
[23] L. Agudo, D. Eyidi, C.H. Schmaranzer, E. Arenholz, N. Jank, J. Bruckner, A.R. Pyzalla, J. Mater. Sci. 42 (2007) 4205.
[24] J.E. Nicholls, Corr. Technol. 11 (1964) 16.
[25] G. Eggeler, W. Auer, H. Kaesche, J. Mater. Sci. 21 (1986) 3348.
[26] E. Gebhardt, W. Obrowski, Z. Metall. 44 (1953) 154.
[27] A.R. Marder, Prog. Mater. Sci. 45 (2000) 191.
[28] L. Fedrizzi, F. Deflorian, S. Ross, Werkst. Korros. 45 (1994) 222.
[29] Z. Panossiana, L. Mariacab, M. Morcilloc, S. Floresd, J. Rochae, J.J. Penaf, F. Herrerag, F. Corvoh, M. Sanchezi, O.T. Rinconj, G. Pridybailok, J. Simancasc, Surf. Coat. Technol. 190 (2005) 244.
[30] J.D. Culcasi, P.R. Sere, C.I. Elsner, A.R. Di Sarli, Surf. Coat. Technol. 122 (1999) 21.
[31] C.E. Albright, Weld. J. (Research Supplement) (1981) 207.
[32] E. Baril, G. L'Esperance, Metall. Mater. Trans. A 30 (1999) 681.
[33] Eggeler G., Ph.D. Thesis, Friedrich Alexander Universität, Erlangen, 1985.
[34] V. Raghavan, J. Phase Equilib. Diffus. 29 (5) (2008).
[35] V. Raghavan, J. Phase Equilib. Diffus. 34 (1) (2013).
[36] P. Perrot, J.C. Tissier, J.Y. Dauphin, Z. Metall. 83 (1992) 786.
[37] A. Bouayad, C. Gerometta, A. Belkebir, A. Ambari, Mater. Sci. Eng. A 363 (2003) 53.
[38] D. Naoi, M. Kajihara, Mater. Sci. Eng. A 459 (2007) 375.
[39] Y.C. Chen, T. Komazaki, T. Tsumura, K. Nakata, Mater. Sci. Technol. 24 (2008) 33.
[40] J.L. Murray, Bull. Alloy Phase Diagrams 4 (1983).
[41] W.F. Gale, D.A. Butts, Sci. Technol. Weld. Joining 9 (2004) 283.
[42] A.D. Smigelkas, E.O. Kirkendall, Trans. AIME 171 (1947) 130.
[43] A.K. Dahle, K. Nogita, S.D. McDonald, C. Dinnis, L. Luc, Mater. Sci. Eng. A 413 (2005) 243.
[44] R. Aparicio, G. Barrera, G. Trapaga, M. Ramirez-Argaez, C. Gonzalez-Rivera, Metall. Mater. Int. 19 (2013) 707.
[45] A. Kouadri-David, Mater. Des. 54 (2014) 184.
[46] A. Elrefaey, M. Takahashi, K. Ikeuchi, Q. J. Jpn. Weld. Soc. 23 (2005).
[47] R.S. Coelho, A. Kostka, J.F. dos Santos, A.R. Pyzalla, Adv. Eng. Mater. 10 (2008) 1127.
[48] R.S. Coelho, A. Kostka, J.F. dos Santos, A. Kaysser-Pyzalla, Mater. Sci. Eng. A 556 (2012) 175.
[49] G.V. Kidson, J. Nucl. Mater. 3 (1961) 21.
[50] R. Lison, Schweissen Schneiden 28 (1976) 89.